VIP

Using Noncovalent Intra-strand and Inter-strand Interactions To Prescribe Helix Formation within a Metallo-supramolecular System

Laura J. Childs, Mirela Pascu, Adam J. Clarke, Nathaniel W. Alcock, and Michael J. Hannon*[a]

Abstract: The effect of inter-strand and intra-strand interactions is explored in a metallo-supramolecular system in which the metal–ligand coordination requirements may be satisfied by more than one different supramolecular architecture. This is achieved by introducing alkyl substituents onto the spacers of readily prepared bis(pyridylimine) ligands. The alkyl substituents induce twisting within the ligand strand and this intra-strand effect favours formation of helical architectures. The alkyl substituents also introduce inter-strand CH···π interactions into the system. For the smaller methyl group these are most effectively accommodated in a trinuclear circular helicate architecture. A solution mixture of dinuclear double-helicate and trinuclear circular helicate results from which, for copper(I), the trinuclear circular helicate crystallises. The CH···π interactions endow the circular helicate with a bowl-shaped conformation and the triangular unit aggregates into a tetrahedral ball-shaped array. Low-temperature NMR studies indicate that the CH···π interactions also confer a bowl-shaped conformation on the triangle in solution. The larger ethyl groups can sustain intra-strand CH···π interactions in the lower nuclearity double-helical system and this is the unique architecture for that ligand system in both solution and the solid state. Crystal structures are described for both the copper(I) and silver(I) complexes. Thus we show that intra-strand interactions may be used to induce helicity within this system, while the nuclearity of the array can be prescribed by the inter-strand interactions.

Keywords: helical structures · N ligands · noncovalent interactions · pi interactions · supramolecular chemistry

Introduction

The design of complex metallo-supramolecular architectures remains an area of intense activity[1,2] driven not only by the aesthetic appeal of the structures but also by emerging applications in diverse areas such as liquid crystals,[3] anion and guest binding[4–6] and DNA recognition.[7,8] Much of our work in this area has focused on routes that allow increasingly complex architectures to be assembled rapidly in one-pot reactions from commercial reagents.[9,10,11a–c,12] Removing the need for extensive synthetic procedures, allows us to focus on probing the structure and activity of the arrays. In particular we have designed metallo-supramolecular cylinders to recognise the major groove of B-DNA and we have demonstrated that they induce unprecedented DNA coiling.[7] These cylinders are triple-stranded helical structures, assembled from the bis(pyridylimine) ligand L^H and octahedral metal ions (Scheme 1).

Helical metallo-supramolecular arrays in particular have attracted much attention.[2] Their design utilises ligands containing multiple metal binding sites whose donor sets are matched to the coordination geometric requirements of specific metals so as to give rise to multi-stranded arrays. The ligand must offer sufficient flexibility for multiple strands to

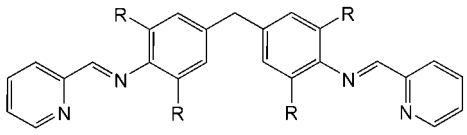

L^H R = H
L^{Me} R = Me
L^{Et} R = Et

Scheme 1. Ligands L^H, L^{Me} and L^{Et}.

[a] Dr. L. J. Childs, M. Pascu, Dr. A. J. Clarke, Dr. N. W. Alcock, Dr. M. J. Hannon
Centre for Supramolecular and Macromolecular Chemistry
Department of Chemistry, University of Warwick
Gibbet Hill Road, Coventry CV4 7AL (UK)
Fax: (+44) 24 7652 4112
E-mail: m.j.hannon@warwick.ac.uk

Supporting information for this article is available on the WWW under http://www.chemeurj.org/ or from the author.

 DOI: 10.1002/chem.200400169

wrap around the two (or more) metal centres, while also being sufficiently rigid to impose the same stereochemistry at both metals. The design can be reinforced by additional inter-strand interactions, but the structure adopted must satisfy the metal–ligand requirements which will be, energetically, the prime interaction in the system.[14] For example, the triple helical structures formed from L^H and octahedral metal ions contain additional interstrand CH···π (face-edge π stacking) interactions which probably contribute to the stability of the array. NMR and X-ray data confirm the presence of these short inter-strand contacts in both solution and the solid-state.

Non-helical isomers arise when the ligand is too flexible to prescribe the same stereochemistry at both metal centres.[13] For example, while the design of L^H is optimal for octahedral metal triple-helix formation, with tetrahedral metal ions a mixture of double-stranded helices (*rac* isomers) and boxes (*meso* isomer) are formed.[10,11] Since in such a system the metal–ligand requirements can be satisfied in more than one way, we decided to explore whether inter-strand or intra-strand interactions could be used to perturb the system and allow access uniquely to the double-helical architecture. The approach bears some relation to our 'frustration' approach in which we have used multiple competing interactions to generate libraries of structures;[14,12] here we use multiple interactions to prescribe a single structure.

Metallo-supramolecular systems in which structure is influenced or prescribed by inter- or intra-strand interactions are rare. Ligand strand design has been used to sterically prevent bis-ligand coordination and thus prescribe heteroligand complexes giving cylinders,[15] rotaxanes,[16] racks[17] and ladders.[18] We have previously reported a double helix in which face-edge π interactions (CH···π) pull two strands together thereby creating a helix with two distinct grooves (major and minor).[11a] Similar effects induced by (face-face) π–π interactions[19] have subsequently been reported by Bermejo and co-workers[20] and more recently by Love and co-workers.[21] In these previous systems the inter-strand interactions influence the precise microarchitecture of the helix but not the global architecture adopted. The system described herein is different in that the inter-strand interactions do influence the nuclearity and architecture of the helical array.

Molecular design: The obvious difference between the *meso* and *rac* conformations formed when L^H interacts with tetrahedral metal ions is the way in which the ligand strands are wrapped around the axis defined by the metal ions (under and over in the helix, over and over in the box).[2] This is illustrated schematically in Figure 1.

These two isomers are in equilibrium in solution and the box is favoured enthalpically, while the helix is favoured by entropy. Thus at low temperature the box dominates but as the temperature is raised the proportion of helix rises (for L^H the copper(I) complex in dichloromethane is a 1:1 mix at 193 K and ~2 helix:1 box at 233 K). In the ^{1}H NMR spectrum the central CH_2 resonances provide a useful handle to identify the two isomers. The CH_2 protons in the helix are equivalent and thus appear as a single resonance, while in the box they are non-equivalent and thus appear as two doublets (see Figure 2).[22] The solid-state structure is dependent on crystallisation conditions and choices of anions and we have crystallographically characterised both helix and box conformations.[10,11]

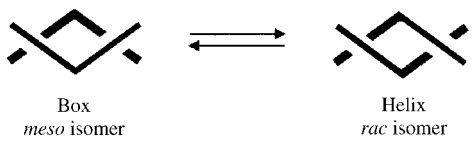

Figure 1. Schematic representation of box and helix conformations.

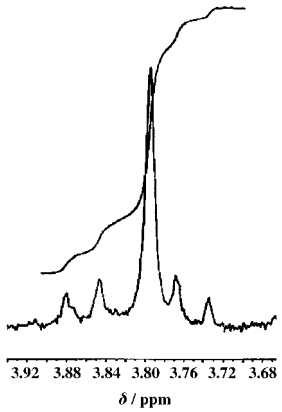

Figure 2. ^{1}H NMR spectrum of central CH_2 resonances showing box and helix species.

A further distinction between the two structures is that in the box architecture the phenyl rings are coplanar with the pyridylimine binding units, while in the helix twisting about the inter-annular bonds is required to facilitate ligand wrapping, as illustrated in Scheme 2.

On the basis of this analysis, the approach that we explore herein to attempt to perturb the box/helix equilibrium is to introduce alkyl groups into the spacer with the goal of (sterically) twisting the phenyl rings out of planarity with the iminopyridine units and thus disfavouring the *meso* isomer.

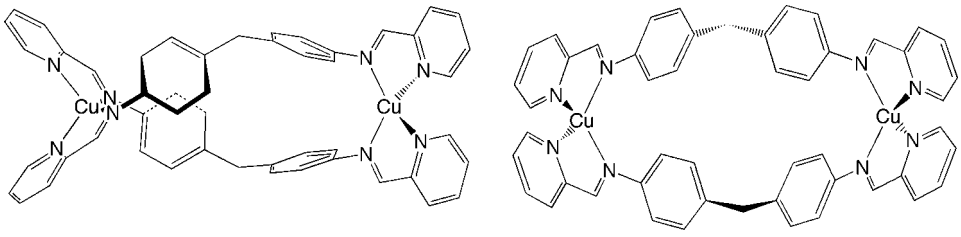

Scheme 2. Schematic representation of helix (left) and box (right) conformations of the dimeric cation $[Cu_2(L^H)_2]^{2+}$.

We report the synthesis of supramolecular arrays from ligands containing methyl and ethyl substituents. These substituents not only disfavour the *meso* isomer, as anticipated, but also introduce new inter-strand CH···π interactions[23] within these double-stranded systems and this can have a dramatic influence on the nuclearity of the helical architecture adopted. An aspect of this work related to L^{Me} has appeared in a preliminary communication focused on controlled aggregation,[24] rather than on inter- and intra-strand interactions which are the focus herein.

Results and Discussion

The ligands L^{Me} and L^{Et} were prepared in $<80\%$ yield by mixing two equivalents of pyridine-2-carboxaldehyde with one equivalent of the appropriate 4,4′-methylenebis(2,6-dialkylaniline) in methanol. The ligand could be isolated and subsequently treated with an appropriate metal salt, or the complexes could be prepared directly in a one-pot reaction by simply mixing aldehyde, diamine and metal salt. Indeed, although not our preferred method, we have established that the copper(I) complex of L^{Me} can be prepared in a solventless reaction by simply grinding the three components in a pestle and mortar.

Complexes of L^{Me}: Reaction of L^{Me} with $[Cu(MeCN)_4][PF_6]$ in methanol yielded a red solution from which a red solid precipitated on cooling. The red colour ($\lambda = 470$ nm, $\varepsilon = 12\,000$ in MeCN) arises from a metal-to-ligand charge transfer (MLCT) transition characteristic of copper(I) in a bis(pyridylimine) environment. To probe whether the methyl groups were sufficient to disfavour the formation of the *meso* isomer, the ^{1}H NMR spectra were recorded in CD_2Cl_2 and CD_3CN solutions. In acetonitrile at room temperature, a single set of resonances are observed but as the temperature is lowered to 233 K, a second species becomes evident in the spectrum. In CD_2Cl_2 at room temperature, two sets of resonances are observed consistent with the presence of two solution species (Figure 3).[25]

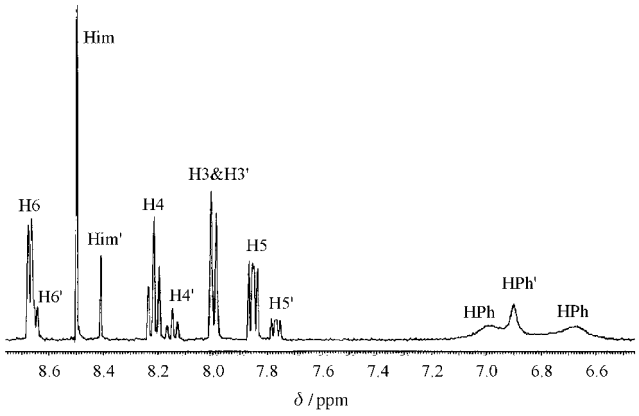

Figure 3. Aromatic region of the ^{1}H NMR spectrum of $[Cu_n(L^{Me})_n][PF_6]_n$ in CD_2Cl_2 at 298 K.

Although two species are present in solution, (as in the unsubstituted compound) in the CH_2 region of the ^{1}H NMR spectrum (Figure 4) two singlets are observed and there is

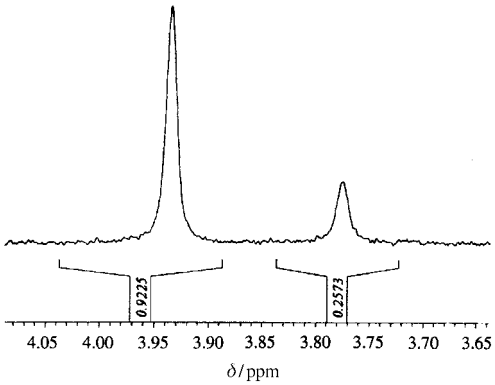

Figure 4. The CH_2 resonances in the ^{1}H NMR spectrum for the copper(I) complexes of L^{Me} in CD_2Cl_2 at 273 K.

no evidence (even at low temperature in dichloromethane) for the pair of doublets characteristic of the CH_2 group in the box (*meso*) architecture (Figure 2). This implies that, as envisaged, the introduction of the methyl group has sterically disfavoured formation of the *meso* isomer. The electrospray mass spectrum shows peaks corresponding to a dimeric species and a trimer. The NMR data coupled with the ESI-MS data leads to the conclusion that the solution species must be a dimeric helix $[Cu_2(L^{Me})_2]^{2+}$ and a (triangular) helical trimer $[Cu_3(L^{Me})_3]^{3+}$.

At 298 K in dichloromethane solution the phenylene protons of the major component are observed as two broad resonances indicating that ring spinning is slow on the NMR time scale. The methyl resonances are observed as a single peak. At lower temperature (273 K) the phenylene resonances have sharpened. Two CH_3 resonances are observed for both species at this temperature. The phenylene protons of the minor component are observed as a singlet at 298 K. By 273 K, two sets of resonances are also observed for these protons. At 213 K, the phenylene protons for the minor species have broadened. At 183 K all the resonances in the spectrum are broadened (possibly due to viscosity effects of solvent at this temperature). However, although all the resonances of the minor component remain broad, two distinct broad signals can be resolved for both the methyl and the CH_2 protons, and new broad peaks just resolved in the baseline in the aromatic region. This implies that the ligand may be unsymmetrically orientated in the complex on the NMR time scale at this temperature.

NMR diffusion experiments in CD_2Cl_2 are consistent with two species of different volume. The major component has a diffusion coefficient of $(1.02 \pm 0.02) \times 10^{-9}\ m^2 s^{-1}$ and the diffusion coefficient of the minor component is $(0.91 \pm 0.02) \times 10^{-9}\ m^2 s^{-1}$. A larger sized species will move more slowly in solution and hence these results indicate that the major component is the smaller (i.e. dimeric) species (see Figure 5).

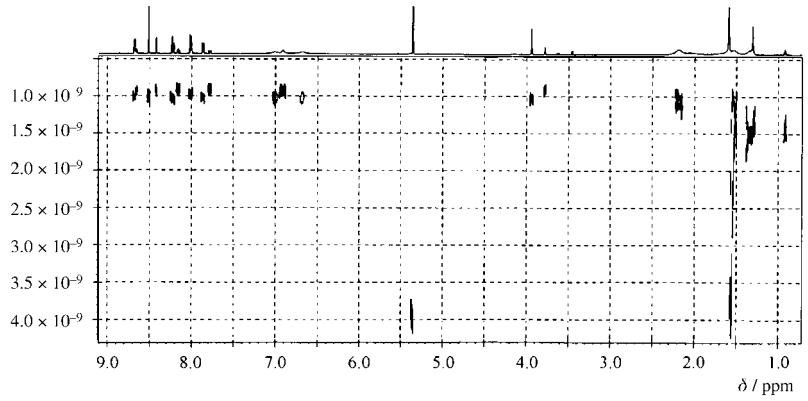

Figure 5. Spectrum of NMR diffusion experiment for copper(I) complexes of ligand L^{Me}.

Recrystallisation of the compound from nitromethane by diffusion of diethyl ether afforded X-ray quality crystals and the X-ray crystal structure has been determined. The solid-state structure reveals a chiral trinuclear circular helicate $[Cu_3(L^{Me})_3]^{3+}$ (Figure 6a).

Each copper(I) centre is bound to two pyridylimine units from two different ligands, and occupies a four-coordinate *pseudo*-tetrahedral environment. The three metal centres prescribe the three vertices of the triangle, and each ligand wraps 'over and under' this triangular plane formed by the three metal ions leading to a trinuclear circular helicate.[26,12] The Cu–$N_{pyridyl}$ distances (2.025(8)–2.067(8) Å) and Cu–N_{imine} distances (2.011(7)–2.049(8) Å) are unremarkable. The pyridylimine–Cu is associated with a typical 'bite angle' of 82.0° and 83.1°. The copper(I) centres are separated by a distance of 11.3 Å. The structure indicates why the methyl groups have induced formation of a trimeric species which was not observed with ligand L^{H}. The methyl groups of one ligand stack above the phenyl rings of an adjacent ligand and a total of six CH–π interactions (CH–centroid 2.9–3.0 Å) are formed within the triangle, that is, six of the twelve methyl groups engage in inter-strand CH–π interactions. These interactions, which would not be possible in a dimeric structure, presumably contribute to the energetic stability and induce formation of this higher order trinuclear structure.

The side view of this trinuclear circular helicate (Figure 6b) reveals that the triangle is not planar but instead slightly bent over towards one face to provide a bowl-shaped motif. This bowl-shaped distortion arises to accommodate the six CH–π interactions and is a consequence of the desire of the methyl groups to form CH–π interactions coupled with the constraints of the ligand connectivity. Thus, these inter-strand interactions not only induce a new architecture but also influence the precise microarchitecture of the array. Three pyridyl rings (one from each ligand) point up towards the cavity of the bowl and are arranged like the blades of a propeller. These 'blades', together with the bowl-shaped topography, have dramatic consequences for the solid-state aggregation of these triangles (Figure 7) as we have previously discussed elsewhere,[24] and four of the bowl-shaped triangular units assemble to form a tetrahedral ball-shaped aggregate through CH–π interactions between the pyridyl rings of the triangles with the phenylene spacers of adjacent triangles. The propeller-type-twist arrangement of the pyridyl 'blades' leads to self-recognition by circular

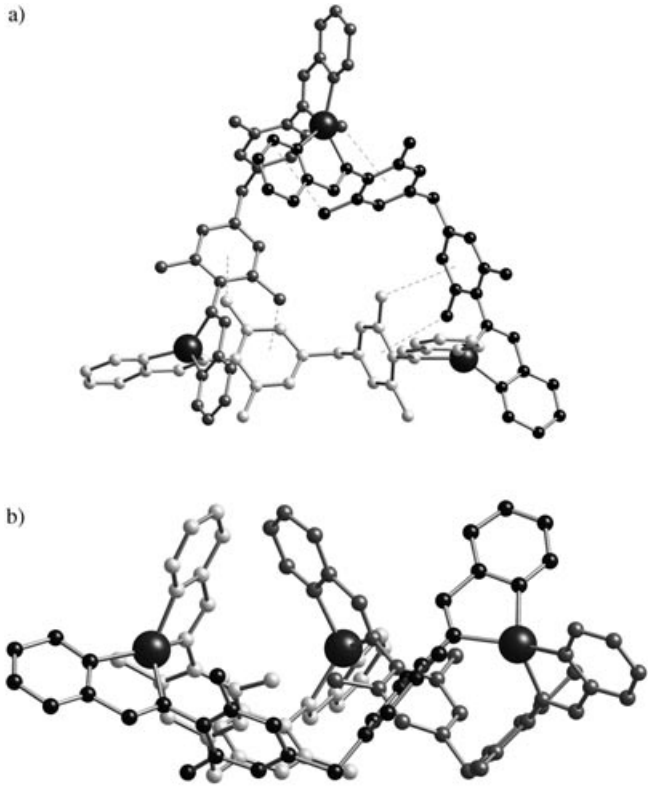

Figure 6. X-ray crystal structure of the $[Cu_3(L^{Me})_3]^{3+}$ ion: a) front view; b) side view. To emphasise the helical nature each ligand is shown in a different shading. Hydrogen atoms are omitted for clarity.

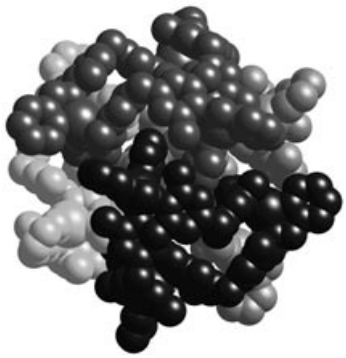

Figure 7. The tetrahedron array resulting from the aggregation of four $[Cu_3(L^{Me})_3]^{3+}$ trimers; each trimer is shaded differently. Hydrogen atoms are omitted for clarity.

helicates of the same chirality giving a chiral tetrahedral ball of ~2.5 nm (C···C) diameter, inside which four PF_6^- counter anions are located.

NMR dilution studies in CD_2Cl_2 over the range 15.5–0.5 mM revealed no change in the positions of the peaks corresponding to either trimer or dimer implying no further aggregation of the triangle (or dimer) into a higher order species at these NMR concentrations. The ratio of the two species varies over these concentration ratios as expected with the proportion of trimer decreasing as the solution becomes more dilute. The difference in free energy, ΔG, between the dimeric and trimeric species was calculated from these dilution studies; an approximate value for ΔG was obtained from 20 different concentrations and the average value calculated to be 8.9 ± 0.2 kJ mol^{-1} K.

The NMR observation that the ligand resonances become non-equivalent at low temperature in dichloromethane would be consistent with the bowl shape starting to freeze out at this temperature.

Reaction of L^{Me} with silver(I) ions: Reaction of ligand L^{Me} with silver(I) acetate yields a yellow solution from which a yellow solid precipitated on treatment with $[NH_4][PF_6]$. ESI mass spectrometry revealed peaks corresponding to $\{Ag_3(L^{Me})_3(PF_6)\}^{2+}$, $\{Ag_3(L^{Me})_3\}^{3+}$, $\{Ag_2(L^{Me})_2(PF_6)\}^{+}$ and $\{Ag_2(L^{Me})_2\}^{2+}$ again consistent with the formation of both dimer and trimer in solution.

The ^{1}H NMR spectra of the compound have been recorded in both CD_2Cl_2 and CD_3CN solution. In CD_3CN at room temperature, a single set of resonances is observed. In CD_2Cl_2 at 283 K, two sets of resonances of almost (but not quite) equal intensity are present indicating two solution species (Figure 8).

For both species the central CH_2 resonance is a singlet consistent with helical dimers and trimers as in the copper(I) complex. In both cases the phenyl and methyl protons are singlets, indicating that ring spinning is fast on the NMR time scale at this temperature. As the temperature is reduced the ratio of the two species varies quite dramatically such that at 223 K the ratio is about 10:1. As the temperature is reduced the phenyl and methyl signals also start to broaden and split into two as ring spinning is slowed. Similar signal broadening and ligand asymmetry at very low temperature are observed as in the copper(I) complex. Although several batches of crystalline material were obtained and investigated, diffraction was very weak.

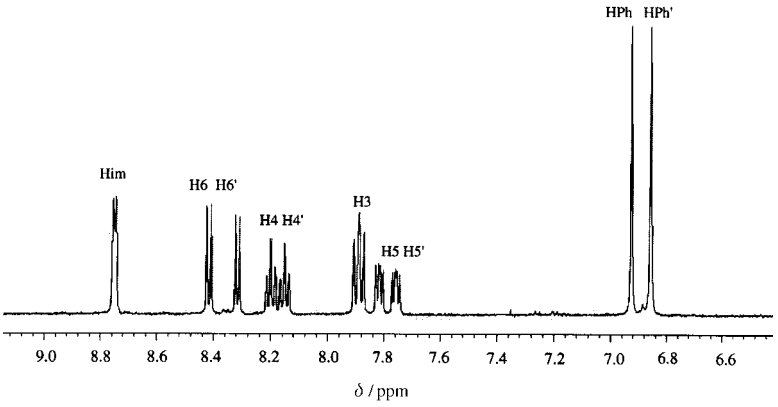

Figure 8. ^{1}H NMR spectrum of $[Ag_n(L^{Me})_n][PF_6]_n$ in CD_2Cl_2 at 283 K.

Ligand L^{Et}: While methyl substitutents were successful in eliminating the *meso* isomer from the equilibrium, they induce an additional trimeric species. The copper(I) crystal structure reveals that this trimeric species allows the ligand to form short CH–π contacts that would not be possible in the dinuclear helical structure. We reasoned that switching to longer ethyl groups in L^{Et} might allow shorter CH···π contacts to be achieved in a double-helical architecture and consequently remove the factor favouring the trimer (a trimer should be disfavoured on entropic grounds). Ligand L^{Et} was therefore prepared. An additional feature of the ethyl substituent is that the ethyl CH_2 unit represents a potentially diastereotopic group which might act as a probe for the presence of chiral helical arrays in solution.

Reaction of L^{Et} with copper(I) ions: Ligand L^{Et} was allowed to react with copper(I) as described for L^{Me}. The mass spectrometry (FAB and ESI) is consistent with a dinuclear formulation $[Cu_2(L^{Et})_2][PF_6]_2$ and there is no evidence for trimeric peaks in the mass spectra. The absorption spectrum in acetonitrile solution shows broad absorptions centred at 275 nm ($\varepsilon = 17\,000$), 339 nm ($\varepsilon = 42\,000$) and 475 nm ($\varepsilon = 1300$). The MLCT transition at 475 nm is again typical of copper(I) in a bis(pyridylimine) environment.

The red solid was recrystallised from acetonitrile by the slow diffusion of benzene to yield red crystals. To determine the solid-state molecular structure an X-ray analysis has been conducted. The solid-state structure confirms that the cation is indeed an M_2L_2 double-helical architecture (Figure 9). Each copper(I) centre is *pseudo*-tetrahedral, coordinating to a pyridylimine binding sub-unit of each ligand. Each ligand strand wraps over and under the plane formed by the metal–metal axis and the stereochemical configuration at each metal centre is identical, giving rise to the helical character. The Cu···Cu intermetallic distance is 11.06 Å. The $Cu–N_{imine}$ (2.034(2)–2.050(2) Å) and the $Cu–N_{pyridine}$ (2.038(2)–2.061(2) Å) distances and the 'bite angles' of 80.9–81.9° are unremarkable. The imines are almost coplanar with the pyridyl rings (dihedral angles of 1.9–4.6°) as is expected and there is dramatic twisting between the pyridylimine units and the aryl rings of the spacer as anticipated in the molecular design (64.3–69.2°). There are four CH···π interactions (CH···centroid 3.71–3.82 Å) within the helicate which occur between the CH_3 units of one ligand and the phenyl rings of the opposite ligand.

The helicates pack together in chains as shown in Figure 10. The structure contains chains of helices of the same chirality

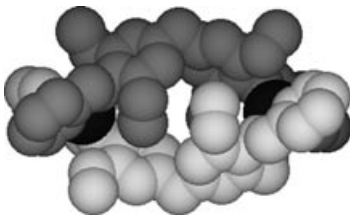

Figure 9. Space-filling representation of the X-ray crystal structure of double-helicate $[Cu_2(L^{Et})_2]^{2+}$. Hydrogen atoms are omitted for clarity.

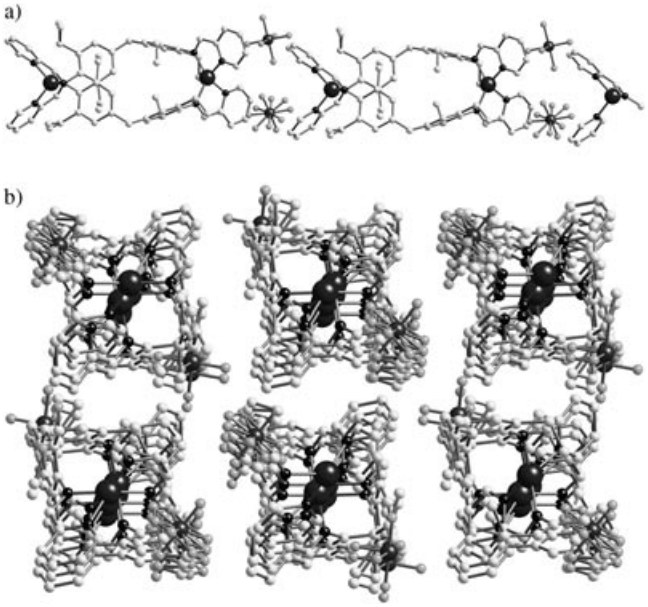

Figure 10. X-ray crystal packing diagram of the $[Cu_2(L^{Et})_2]^{2+}$ cations. a) Chain structure ; b) perpendicular view illustrating the packing of chains. Hydrogen atoms are omitted for clarity.

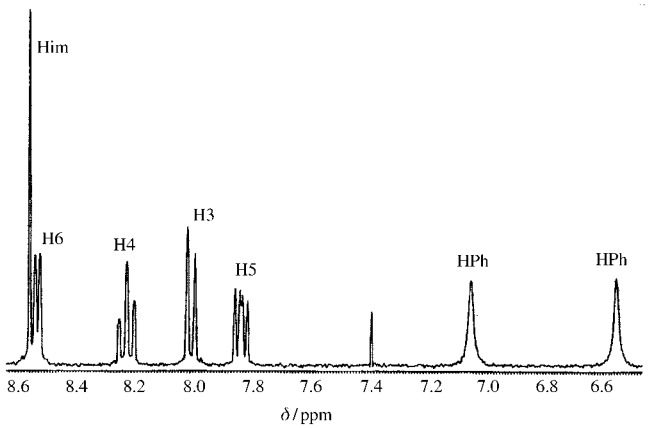

Figure 11. Aromatic region of ^{1}H NMR spectrum of $[Cu_2(L^{Et})_2][PF_6]_2$ in CD_2Cl_2 at 298 K.

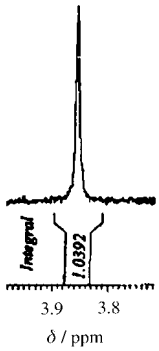

Figure 12. Central CH_2 resonance of $[Cu_2(L^{Et})_2][PF_6]_2$ at 298 K in CD_2Cl_2.

packed into a grid-like arrangement with chirality alternating in adjacent chains and rendering the overall structure achiral. The hexafluorophosphate anions are incorporated into the chains, packed between the helicates.

To establish that the double helical architecture is retained in solution and is the only solution species, the ^{1}H NMR spectra of the complex at room temperature have been recorded in both CD_3CN and CD_2Cl_2 (Figure 11).

In both cases, only a single set of resonances are observed, and in both cases the central CH_2 resonance is a singlet implying formation of a helical array (Figure 12).

As the temperature is reduced to 183 K a single set of resonances is still observed in the CD_2Cl_2 spectrum confirming the presence of just a single solution species of helical nature. Coupled with the electrospray mass spectra data this species must be a dinuclear double helicate. The chiral nature of the species is confirmed by the observation that the ethyl CH_2 protons are non-equivalent (Figure 13).

Ring spinning is slow and so four resonances are observed for these protons, that is, both of the (diastereotopic) ethyl CH_2 groups become non-equivalent. Two of the protons are deshielded ($\delta = \sim 2$, ~ 2.1 ppm) compared to the free ligand ($\delta = \sim 2.5$ ppm in ligand) and the other two resonances ($\delta = \sim 2.6$, 2.7 ppm) are not deshielded. Similarly, two distinct methyl groups are observed at low temperature ($\delta = \sim 1.1$ and ~ 0.5 ppm) and one is deshielded compared to the free ligand ($\delta = 1.1$ ppm). Such deshielding is consistent with the group lying above an aromatic ring π-stacked as in the crystal structure. A 2D NOESY experiment indicates that this deshielded methyl (~ 0.5 ppm) is attached to the two deshielded CH_2 protons which would also be located above the ring. The shifts are thus consistent with the retention of the π-stacked structure in solution as in the solid state. As the temperature drops these shielded resonances start to broaden but within the available temperature ranges do not split.

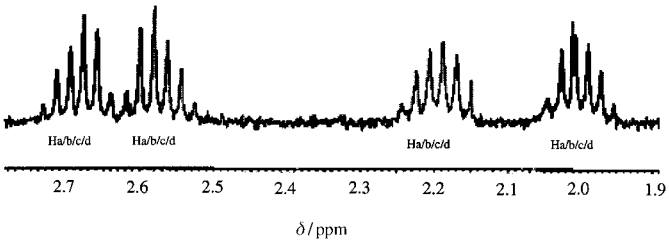

Figure 13. NMR expansion of the region showing diastereotopic resonances of H_a to H_d of $[Cu_2(L^{Et})_2][PF_6]_2$ in CD_2Cl_2 at 273 K.

Reaction of L^{Et} with silver(I) ions: Ligand L^{Et} was allowed to react with silver(I) acetate in the same way as described for ligand L^{Me}. Mass spectra (FAB and ESI) are consistent with the formation of a dimeric species of formula $[Ag_2(L^{Et})_2][PF_6]_2$.

Yellow crystals were obtained from acetonitrile by the slow diffusion of diethyl ether. The crystals were suitable for X-ray diffraction studies and this allowed the solid-state molecular architecture to be determined. As in the copper(I) complex, a double helicate is formed (Figure 14).

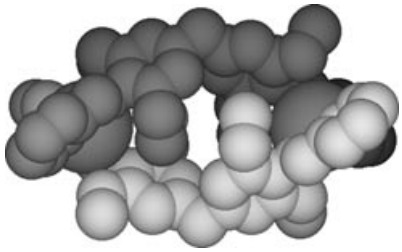

Figure 14. Space-filling representation of the X-ray crystal structure of double-helicate $[Ag_2(L^{Et})_2]^{2+}$. Hydrogen atoms are omitted for clarity.

Each silver(I) centre is pseudo-tetrahedral, coordinating to a pyridylimine binding sub-unit of each ligand. Each ligand strand wraps over and under the plane formed by the metal–metal axis. The Ag–Ag intermetallic distance is 11.38 Å. The $Ag–N_{imine}$ (2.315(3)–2.367(3) Å) and $Ag–N_{pyridine}$ (2.261(4)–2.304(4) Å) distances and the bite angles of 72.8–73.4° are unremarkable. The imines are again almost coplanar with the pyridyl rings (dihedral angles of 0.3–2.3°) and the twisting necessary for helicate formation occurs between the pyridylimine units and the phenyl spacers. There are four CH···π interactions (CH···centroid 3.56–3.81 Å) within the helicate, analogous to those in the copper helicate, between the ethyl groups of one ligand and the phenyl rings of an opposite ligand. The crystal packing of these silver(I) helicates is entirely analogous to the packing of the copper(I) helicates (see Supporting Information).

Once again, ^{1}H NMR spectroscopy in CD_3CN and CD_2Cl_2 indicated a single solution species of helical architecture (central CH_2 is a singlet) in solution even at low temperatures (Figure 15). At room temperature in CD_2Cl_2 a Ag-imine splitting of 8.3 Hz is observed confirming coordination.

In contrast to the room-temperature spectrum of the copper complex, in the spectrum of the silver complex the phenylene protons resonate as a singlet indicating that the phenylene rings are spinning rapidly on the NMR time scale. Similarly single methyl and CH_2 (ethyl) resonances are observed. As the temperature is lowered, the ring-spinning process freezes out and two phenyl, two methyl and three ethyl CH_2 resonances (corresponding to four signals, two of which overlap) are observed. As in the copper complex one of each of the phenyl and methyl resonances is deshielded implying again that the CH···π interactions observed in the crystal are retained in solution. At coalescence (~245 K) the rate of ring spinning is estimated to be 400 Hz. The more facile ring spinning in this silver complex may be a consequence of the longer silver–N bond lengths and consequent inter-spacer separation.

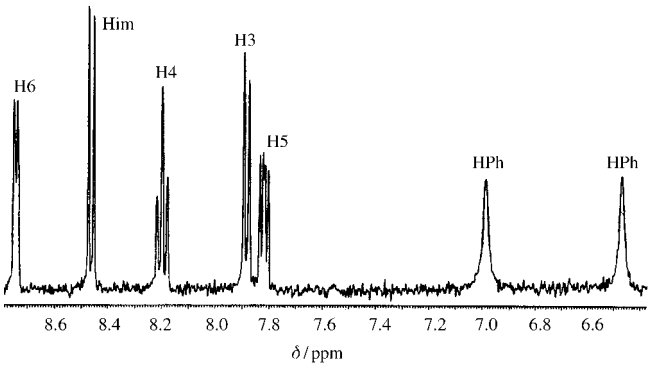

Figure 15. Aromatic region of ^{1}H NMR spectrum of $[Ag_2(L^{Et})_2][PF_6]_2$ in CD_2Cl_2 at 233 K.

Conclusion

We have demonstrated that alkyl substituents introduced into the spacer can indeed induce strand twisting and thus disfavour box (*meso* isomer) formation. However, these alkyl substituents introduce secondary non-covalent interactions into the strand and these reveal themselves in inter-strand processes which can dramatically influence the architectures assembled. Thus the methyl groups introduce a new architecture into the solution library of potential structures (a trinuclear circular helicate) as a consequence of inter-strand CH···π interactions. A mixture of dinuclear double-helicate and trinuclear circular helicate thus arises. For longer ethyl substituents such CH···π interactions can already be achieved within the dinuclear double-helicate and so the higher order (and thus entropically disfavoured) trinuclear circular helicate is not observed (the longer ethyl group may also be too long to form effective CH···π interactions within the trinuclear system). In this system the ethyl substituents, and the non-covalent and steric interactions they introduce, prescribe and direct the exclusive formation of a double helical array. A consequence of the CH···π interactions in the trinuclear circular helicate is the induction of a bowl-shaped configuration in the solid state. NMR solution studies indicate that a similar conformation may also be adopted in solution, although this is dynamic and only starts to freeze out at very low temperature. In the solid state the bowl-shaped topography leads to aggregation into a tetrahedral ball-shaped array at the heart of which lie hexafluorophosphate anions which make a number of short contacts and probably contribute to the stabilisation of this supramolecular aggregate. Thus secondary non-covalent inter-strand interactions can play a powerful role in determining metallo-supramolecular architectures.

Experimental Section

General: All starting materials and reagents were purchased from Aldrich and used without further purification. ^{1}H NMR studies were carried out on DPX 300, ACP 400 or DRX 500 MHz Bruker spectrometers using standard Bruker software. Infra-red spectra were recorded on a Nicolet Avalar FTIR as compressed solid pellets or as compressed KBr pellets. FAB, EI and CI mass spectra were recorded at the University of Warwick

on a Micromass Autospec spectrometer. ESI mass spectra were recorded on Micromass Quatro II (low resolution triple quadrupole mass spectrometer) instruments at the EPSRC National Mass Spectrometry Centre, University of Wales, Swansea. Elemental analysis was performed by Warwick Analytical Services on a Leeman Labs CE44 CHN analyser. UV/Vis measurements were made using a PU 8720 scanning spectrometer or a Jasco V-550 spectrophotometer. X-ray data was collected with a Siemens SMART three-circle system with a CCD area detector and refinement performed using SHELXL 97.[27]

Synthesis of ligands L^{Me} and L^{Et}: Ground 3 Å dried molecular sieves (5 g) and 4,4′-methylenebis(2,6-diethylaniline) or 4,4′-methylenebis(2,6-dimethylaniline) (0.678 g, 2.67 mmol) were added to methanol (90 mL) and stirred under a nitrogen atmosphere until the methylenedianaline had dissolved (approximately 5 min). Pyridine-2-carboxyaldehyde (0.571 g, 5.34 mmol) was added and the mixture stirred at room temperature for 24 h. The molecular sieves were removed by filtration and the filtrate concentrated by rotary evaporation to produce a yellow solid.

L^{Me}: Yellow solid (0.934 g, 81 %). IR (KBr): $\tilde{\nu}$ = 2996w, 2905 m, 2846w, 1638 s, 1583 m, 1476 s, 1433 s, 1385 s, 1318w, 1283w, 1200 s, 1141 m, 1089w, 1042w, 987 m, 876 m, 837 m, 774 s, 742 m, 695w, 647w, 616w cm^{-1}; MS (+ve CI): *m/z*: 433 $[M+H]^+$; elemental analysis calcd (%) for $C_{29}H_{28}N_4$: C 80.5, H 6.5, N 13.0; found: C 80.5, H 6.6, N 13.0; ^1H NMR ($CDCl_3$): δ = 8.72 (d, J = 4.9 Hz, 1H; H_6), 8.35 (s, 1H; H_i), 8.28 (d, J = 7.9 Hz, 1H; H_3), 7.84 (td, J = 7.9, 1.7 Hz, 1H; $H_{4/5}$), 7.40 (ddd, J = 7.5, 4.7, 1.1 Hz, 1H; $H_{4/5}$), 6.94 (s, 2H; H_{Ph}), 3.85 (s, 1H; central CH_2), 2.15 ppm (s, 6H; CH_3); ^{13}C NMR ($CDCl_3$): δ = 163.83 (C_7), 154.94 ($C_{2/8/11}$), 149.99 (C_6), 148.76 ($C_{2/8/11}$), 137.53 ($C_{2/8/11}$), 137.11 ($C_{4/5}$), 129.11 (C_{10} & C_{12}), 127.43 (C_9 & C_{13}), 125.68 ($C_{4/5}$), 121.59 (C_3), 41.28 (C_{16}), 18.79 ppm (C_{14} & C_{15}).

L^{Et}: From 4,4′-methylenebis(2,6-diethylaniline) (4.087 g, 13.16 mmol) and pyridine-2-carboxyaldehyde (2.820 g, 26.33 mmol). Yellow solid (5.459 g, 85 %). IR (KBr): $\tilde{\nu}$ = 2953 s, 2925 s, 2862 s, 1642 s, 1587 s, 1563 s, 1468 s, 1456 s, 1433 s, 1381w, 1362w, 1338w, 1314w, 1291 m, 1220w, 1192 s, 1141 s, 1078w, 995 s, 936 m, 892 m, 853 s, 770 s, 742 m, 691w, 659 m cm^{-1}; elemental analysis calcd (%) for $C_{33}H_{36}N_4 \cdot 0.5\,CH_3OH$: C 79.7, H 7.6, N 11.1; found: C 80.0, H 7.4, N 11.4; MS (+ve EI): *m/z* 488 $[M]^+$; ^1H NMR ($CDCl_3$): δ = 8.72 (dq, J = 4.9, 0.9 Hz, 1H; H_6), 8.35 (s, 1H; H_i), 8.27 (dt, J = 7.7, 1.1 Hz, 1H; H_3), 7.85 (td, J = 7.5, 1.1 Hz, 1H; $H_{4/5}$), 7.41 (ddd, J = 7.5, 4.9, 1.1 Hz, 1H; $H_{4/5}$), 6.97 (s, 2H; H_{Ph}), 3.94 (s, central CH_2; 1H), 2.50 (q, J = 7.5 Hz, 4H; CH_2), 1.13 ppm (t, J = 7.5 Hz, 6H; CH_3); ^{13}C NMR ($CDCl_3$): δ = 163.46 (C_7), 154.92 ($C_{2/8/11}$), 150.00 (C_6), 147.96 ($C_{2/8/11}$), 137.57 ($C_{2/8/11}$), 137.15 ($C_{4/5}$), 133.30 (C_9 & C_{13}), 127.34 (C_{10} & C_{12}), 125.67 ($C_{4/5}$), 121.59 (C_3), 41.54 (C_{18}), 25.11 (C_{14} & C_{16}), 15.18 ppm (C_{15} & C_{17}).

Synthesis of $[Cu_n(L^{Me})_n][PF_6]_n$: Ligand L^{Me} (0.084 g, 0.19 mmol) was dissolved in methanol and whilst stirring under a nitrogen atmosphere, $[Cu(MeCN)_4][PF_6]$ (0.072 g, 0.19 mmol) was added to give a dark red solution. The solution was heated under reflux overnight and then cooled to room temperature. A black solid precipitated from the solution on standing. This was collected by filtration and washed with diethyl ether (0.173 g, 71 %). X-ray quality crystals were obtained by the slow diffusion of diethyl ether into a solution of the complex in nitromethane.

The same compound can be prepared in a single pot simply by mixing the aldehyde and diamine and then adding the cuprous salt. It can also be prepared in a solventless reaction by grinding the three compounds together.

IR (KBr): $\tilde{\nu}$ = 2902w, 1586 m, 1474 m, 1440 m, 1380 m, 1303w, 1200 m, 1140w, 900w, 836 s, 772 m, 742w, 558 m cm^{-1}; MS (ESI): *m/z* 1135 $\{Cu_2(L^{Me})_2(PF_6)\}^+$, 927 $\{Cu(L^{Me})_2\}^+$, 816 $\{Cu_3(L^{Me})_3(PF_6)\}^{2+}$, 495 $\{Cu_2(L^{Me})_2\}^{2+}$, $\{Cu(L^{Me})\}^+$; MS (+ve FAB): *m/z*: 1137 $[Cu_2(L^{Me})_2(PF_6)]^+$, 495 $[Cu_2(L^{Me})_2]^+$; ^1H NMR: (CD_2Cl_2): δ = 8.67 (d, J = 4.9 Hz, 4H; H_6), 8.49 (s, 3H; H_i *helix*), 8.40 (s, 1H; H_i, *trimer*), 8.21 (td, J = 7.7, 1.5 Hz, 3H; H_4 *helix*), 8.15 (td, J = 7.7, 1.5 Hz, 1H; H_4 *trimer*), 7.99 (d, J = 7.9 Hz; 4H, H_3), 7.85 (ddd, J = 7.7, 5.1, 1.3 Hz, 3H; H_5 *helix*), 7.77 (ddd, J = 7.7, 5.1, 1.3 Hz, 1H; H_5 *trimer*), 6.99 (s, 3H; H_{Ph} *helix*), 6.90 (s, 2H; H_{Ph} *trimer*), 6.67 (s, 3H; H_{Ph} *helix*), 3.92 (s, 3H; central CH_2 *helix*), 3.76 (s, 1H; central CH_2 *trimer*), 2.04 ppm (br. s, 24H; CH_3); UV/Vis (MeCN): λ = 470 (ε = 12 000), 334 (ε = 28 000), 328 nm (ε = 75 000).

Synthesis of $[Cu_2(L^{Et})_2][PF_6]_2$: Ligand L^{Et} (0.107 g, 0.284 mmol) was dissolved in methanol and whilst stirring under a nitrogen atmosphere, $[Cu(MeCN)_4][PF_6]$ (0.106 g, 0.284 mmol) was added to give a dark red solution. The solution was heated under reflux overnight and then cooled to room temperature. A dark red solid precipitated from the solution on standing and was collected by filtration and dried with diethyl ether (0.336 g, 85 %). The solid was recrystallised from acetonitrile by the slow diffusion of benzene to afford dark red crystals. IR (KBr): $\tilde{\nu}$ = 2965 m, 2927w, 2867w, 1611 m, 1586 m, 1556w, 1504w, 1470 m, 1436 m, 1380 m, 1303 m, 1252w, 1192 m, 1145 m, 836 s, 772 m, 738w, 549 s cm^{-1}; MS (ESI): *m/z*: 1247 $\{Cu_2(L^{Et})_2(PF_6)\}^+$, 1040 $\{Cu_2(L^{Et})(PF_6)\}^+$, 551 $\{Cu_2(L^{Et})_2\}^{2+}$; MS (+ve FAB): *m/z*: 1247 $[Cu_2(L^{Et})_2(PF_6)]^+$; elemental analysis calcd (%) for $Cu_2C_{66}H_{72}N_8P_2F_{12} \cdot H_2O$: C 56.1, H 5.3, N 7.9; found: C 56.0, H 5.2, N 7.9; ^1H NMR (CD_2Cl_2): δ = 8.56 (s, 1H; H_i), 8.53 (br. d, J = 4.9 Hz, 1H; H_6), 8.22, (td, J = 7.9, 1.4 Hz, 1H; H_4), 8.00 (br. d, J = 7.4 Hz, 1H; H_3), 7.83 (ddd, J = 7.8, 4.9, 1.4 Hz, 1H; H_5), 7.03 (br. d, J = 1.4 Hz, 2H; H_{Ph}), 6.52 (br. d, J = 1.5 Hz, 2H; H_{Ph}), 3.86 (s, 1H; central CH_2), 2.68 (m, 2H; CH_2), 2.58 (m, 2H; CH_2), 2.19 (m, 2H; CH_2), 2.00 (m, 2H; CH_2), 1.02 (t, J = 7.9, 3H; CH_3), 0.45 ppm (t, J = 7.4, 3H; CH_3); UV/Vis (MeCN): λ = 475 (ε = 1300), 339 (ε = 42000), 275 nm (ε = 17 000).

Synthesis of $[Ag_n(L^{Me})_n][PF_6]_n$: Care was taken to exclude light during the following procedure. L^{Me} (0.1 g, 0.231 mmol) was dissolved in chloroform and silver(I) hexafluorophosphate (0.058 g, 0.231 mmol) dissolved in methanol was added and stirred at room temperature for 2 h. The yellow precipitate was collected by vacuum filtration, washed with chloroform and dried in vacuo under P_4O_{10} (0.22 g, 70 %). IR (KBr): $\tilde{\nu}$ = 2923 m, 2855w, 1643 m, 1586 m, 1478 m, 1439 m, 1386 m, 1303w, 1260w, 1197w, 1143w, 1007w, 842 s, 770 m, 741w cm^{-1}; MS (ESI): *m/z*: 1225 $\{Ag_2(L^{Me})_2(PF_6)\}^+$, 973 $\{Ag(L^{Me})_2\}^+$, 883 $\{Ag_3(L^{Me})_3(PF_6)\}^{2+}$, 540 $\{Ag_3(L^{Me})_3\}^{3+}$, $\{Ag_2(L^{Me})_2\}^{2+}$; elemental analysis calcd (%) for $Ag_2C_{58}H_{56}N_8P_2F_{12} \cdot 2H_2O$: C 49.6, H 4.3, N 8.0; found: C 49.4, H 4.1, N 7.8; ^1H NMR (CD_2Cl_2, 283 K): δ = 8.75 (s, 2H; H_i), 8.41 (d, J = 7.5 Hz, 1H; H_6 *helix*), 8.31 (d, J = 6.5 Hz, 1H; H_6 *trimer*), 8.20 (td, J = 7.8, 1.5 Hz, 1H; H_4 *helix*), 8.15 (td, J = 7.8, 1.5 Hz, 1H; H_4 *trimer*), 7.88 (dd, J = 9.7, 7.8 Hz, 2H; H_3), 7.81 (ddd, J = 7.8, 5.0, 2.8 Hz, 1H; H_5 *helix*), 7.81 (ddd, J = 7.8, 5.0, 2.8 Hz, 1H; H_5 *trimer*), 6.92 (s, 2H; H_{Ph} *helix*), 6.85 (s, 2H; H_{Ph} *trimer*), 3.92 (s, 1H; central CH_2 *helix*), 3.76 (s, 1H; central CH_2 *trimer*), 1.94 (s, 6H; CH_3 *helix*), 1.77 ppm (s, 6H; CH_3 *trimer*).

Synthesis of $[Ag_2(L^{Et})_2][PF_6]_2$: Ligand L^{Et} (0.106 g, 0.217 mmol) was dissolved in methanol and whilst stirring under a nitrogen atmosphere and excluding light, silver(I)acetate (0.036 g, 0.217 mmol) was added to give a yellow solution. The solution was heated under reflux in the dark for 1 h and then cooled to room temperature. The solution was filtered through celite and the yellow filtrate collected. A yellow solid precipitated on addition of excess methanolic $[NH_4][PF_6]$ to the filtrate and was collected by filtration (0.238 g, 74 %). X-ray quality crystals were obtained by the slow diffusion of diethyl ether into a solution of the complex in acetonitrile. IR (KBr): $\tilde{\nu}$ = 2964 m, 2928 m, 2870w, 1643 s, 1571w, 1473 m, 1432w, 1384 s, 1309w, 1258w, 1196w, 1145w, 1104 m, 903 m, 838 s, 775w, 611w cm^{-1}; MS (ESI): *m/z*: 1338 $\{Ag_2(L^{Et})_2(PF_6)\}^+$, 1083 $\{Ag(L^{Et})_2\}^+$, 551 $\{Ag_2(L^{Et})_2\}^{2+}$; MS (+ve FAB): *m/z*: 1338 $[Ag_2(L^{Et})_2(PF_6)]^+$; elemental analysis calcd for $Ag_2C_{50}H_{40}N_8P_2F_{12} \cdot H_2O$: C 52.9, H 5.0, N 7.5; found: C 52.8, H 4.9, N 7.3; ^1H NMR (CD_2Cl_2): δ = 8.73 (d, J = 4.9 Hz, 1H; H_6), 8.47 (d, J = 8.3 Hz, 1H; H_i), 8.22 (td, J = 7.7, 1.7 Hz, 1H; H_4), 7.89 (d, J = 7.7 Hz, 1H; H_3), 7.83 (dd J = 7.5, 4.7, Hz, 1H; H_5), 6.71 (s, 2H; H_{Ph}), 3.79 (s, 1H; central CH_2), 2.31 (m, 4H; CH_2), 0.72 ppm (t, J = 7.4 Hz, 6H; CH_3).

X-ray crystallographic structural characterisations

$[Cu_2(L^{Et})_2][PF_6]_2$: Crystal structure data for $C_{66}H_{72}N_8Cu_2P_2F_{12}$, M_r = 1394.34, triclinic, space group $P\bar{1}$, a = 14.4010(2), b = 14.9535(3), c = 17.5995(4) Å, α = 110.1550(10), β = 104.02, γ = 101.6300(10)°, V = 3278.38(11) Å^3, T = 180(2) K, λ = 0.71073, Z = 2, ρ_{calcd} = 1.412 Mg m^{-3}, $F(000)$ = 1440, $\mu(Mo_{K\alpha})$ = 0.778 mm^{-1}. Crystal character: red plates. Crystal dimensions: 0.7 × 0.6 × 0.02 mm, data collected with a Siemens SMART three-circle system with CCD area detector.[28] The crystal was held at 180(2) K with an Oxford Cryosystem Cryostream Cooler;[29] θ_{max} = 29.13°. A total of 20698 reflections was measured, 14848 unique [R_{int} = 0.0173]. Absorption correction by Psi-scan. Weighting scheme $w = 1/[\sigma^2(F_o^2) + (0.0383P)^2]$, where $P = (F_o^2 + 2F_c^2)/3$. Goodness-of-fit on F^2 was 1.045, $R1$ [for 14848 reflections with $I > 2\sigma(I)$] = 0.0441, $wR2$ = 0.1101, data/restraints/parameters 14848/34/877. Largest difference Fourier peak and hole 0.870 and −0.650 e Å^{-3}, respectively. Refinement used SHELXL 97.[27]

$[Ag_2(L^{Et})_2][PF_6]_2$: Crystal structure data for $C_{66}H_{72}N_8Ag_2P_2F_{12}$, M_r = 1483.00, triclinic, space group $P\bar{1}$, a = 14.4970(2), b = 15.19950(10), c = 17.36010(10) Å, α = 108.4720(10), β = 105.1710(10), γ = 99.76°, V = 3365.90(5) Å^3, T = 180(2) K, λ = 0.71073, Z = 2, ρ_{calcd} = 1.463 Mgm^{-3}, $F(000)$ = 1512, $\mu(Mo_{K\alpha})$ = 0.708 mm^{-1}. Crystal character: yellow blocks. Crystal dimensions: 0.5 × 0.3 × 0.3 mm, data collected with a Siemens SMART three-circle system with CCD area detector.[28] The crystal was held at 180(2) K with an Oxford Cryosystem Cryostream Cooler;[29] θ_{max} = 29.10°. A total of 22365 reflections was measured, 15449 unique [R_{int} = 0.0296]. Absorption correction by Psi-scan. Weighting scheme $w = 1/[\sigma^2(F_o^2) + (0.0383P)^2]$, where $P = (F_o^2 + 2F_c^2)/3$. Goodness-of-fit on F^2 was 1.164, $R1$ [for 15449 reflections with $I > 2\sigma(I)$] = 0.0633, $wR2$ = 0.1175, data/restraints/parameters 15449/0/822. Largest difference Fourier peak and hole 0.955 and −0.728 eÅ^{-3}, respectively. Refinement used SHELXL 97.[27]

CCDC-231266 and CCDC-231267 contain the supplementary crystallographic data for this paper. These data can be obtained free of charge via www.ccdc.cam.ac.uk/conts/retrieving.html (or from the Cambridge Crystallographic Data Centre, 12, Union Road, Cambridge CB21EZ, UK; fax: (+44) 1223-336-033; or deposit@ccdc.cam.ac.uk).

The crystal structure data for $[Cu_3(L^{Me})_3][PF_6]_3$ has previously been communicated[24] and is available in the CCDB (ref. LULJIL).

Acknowledgement

This work was supported by the University of Warwick (L.J.C.) and the European Union (Marie Curie Training Site in Supramolecular and Macromolecular Chemistry; HPMT-CT-2001–00365: M.P.). M. J. H. is the Royal Society of Chemistry Sir Edward Frankland Fellow 2004/05. We thank EPSRC and Siemens Analytical Instruments for grants in support of the diffractometer and the EPSRC National Mass Spectrometry Centre, Swansea for recording some of the mass spectra.

[1] a) J.-M. Lehn, *Supramolecular Chemistry - Concepts and Perspectives*, VCH, Weinheim, **1995**; b) *Comprehensive Supramolecular Chemistry*, (Eds.: J. L. Atwood, J. E. D. Davies, J.-M. Lehn, D. D. MacNicol, F. Vogtle), Pergamon, Oxford, **1996**; c) R. W. Saalfrank, I. Bernt, *Curr. Opin. Solid State Mater. Sci.* **1998**, *3*, 407–413; d) D. Philp, J. F. Stoddart, *Angew. Chem.* **1996**, *108*, 1242–1286; *Angew. Chem. Int. Ed. Engl.* **1996**, *35*, 1154–1196; e) M. Albrecht, *J. Inclusion Phenom. Macrocyclic Chem.* **2000**, *36*, 127–151; f) A. F. Williams, *Pure Appl. Chem.* **1996**, *68*, 1285–1289; g) C. Dietrich-Buchecker, G. Rapenne, J. P. Sauvage, *Coord. Chem. Rev.* **1999**, *186*, 167–176; h) M. Fujita, *Acc. Chem. Res.* **1999**, *32*, 53–61; i) B. Olenyuk, A. Fechtenkotter, P. J. Stang, *J. Chem. Soc. Dalton Trans.* **1998**, 1707–1728; j) D. L. Caulder, K. N. Raymond, *Acc. Chem. Res.* **1999**, *32*, 975–982; k) D. W. Johnson, K. N. Raymond, *Supramol. Chem.* **2001**, *13*, 639–659; l) E. C. Constable, *Prog. Inorg. Chem.* **1994**, *42*, 67–138; m) R. W. Saalfrank, I. Bernt, *Curr. Opin. Solid State Mater. Sci.* **1998**, *3*, 407–413.

[2] a) L. J. Childs, M. J. Hannon, *Supramol. Chem.* **2004**, *16*, 7–22; b) C. Piguet, G. Bernardinelli, G. Hopfgartner, *Chem. Rev.* **1997**, *97*, 2005–2062; c) M. Albrecht, *Chem. Rev.* **2001**, *101*, 3457–3497.

[3] a) A. El-ghayoury, L. Douce, A. Skoulios, R. Ziessel, *Angew. Chem.* **1998**, *110*, 2327–2331; *Angew. Chem. Int. Ed.* **1998**, *37*, 2205–2208; b) L. Douce, R. Ziessel, *Mol. Cryst. Liq. Cryst.* **2001**, *362*, 133–145; c) R. Ziessel, *Coord. Chem. Rev.* **2001**, *216*, 195–223.

[4] a) A. Bilyk, M. M. Harding, *J. Chem. Soc. Dalton Trans.* **1994**, 77–82; b) A. Bilyk, M. M. Harding, P. Turner, T. W. Hambley, *J. Chem. Soc. Dalton Trans.* **1995**, 2549–2553; c) A. Bilyk, M. M. Harding, *J. Chem. Soc. Chem. Commun.* **1995**, 1697–1698; d) M. A. Houghton, A. Bilyk, M. M. Harding, P. Turner, T. W. Hambley, *J. Chem. Soc. Dalton Trans.* **1997**, 2725–2733.

[5] M. Albrecht, O. Blau, *Chem. Commun.* **1997**, 345–346.

[6] B. Hasenknopf, J.-M. Lehn, B. O. Kneisel, G. Baum, D. Fenske, *Angew. Chem.* **1996**, *108*, 1987–1989; *Angew. Chem. Int. Ed. Engl.* **1996**, *35*, 1838–1840.

[7] a) M. J. Hannon, V. Moreno, M. J. Prieto, E. Molderheim, E. Sletten, I. Meistermann, C. J. Isaac, K. J. Sanders, A. Rodger, *Angew. Chem.* **2001**, *113*, 903–908; *Angew. Chem. Int. Ed.* **2001**, *40*, 880–884; b) I. Meistermann, V. Moreno, M. J. Prieto, E. Moldrheim, E. Sletten, S. Khalid, M. Rodger, J. Peberdy, C. J. Isaac, A. Rodger, M. J. Hannon, *Proc. Natl. Acad. Sci. USA* **2002**, *99*, 5069–5074; c) E. Moldrheim, M. J. Hannon, I. Meistermann, A. Rodger, E. Sletten, *J. Biol. Inorg. Chem.* **2002**, *7*, 770–780; d) M. J. Hannon, A. Rodger, *Pharmaceutical Visions* **2002**, autumn issue, 14–16.

[8] B. Schoentjes, J. -M. Lehn, *Helv. Chim. Acta* **1995**, *78*, 1–12.

[9] a) M. J. Hannon, S. Bunce, A. J. Clarke, N. W. Alcock, *Angew. Chem.* **1999**, *111*, 1353–1355; *Angew. Chem. Int. Ed.* **1999**, *38*, 1277–1278; b) L. J. Childs, N. W. Alcock, M. J. Hannon, *Angew. Chem.* **2001**, *113*, 1113–1115; *Angew. Chem. Int. Ed.* **2001**, *40*, 1079–1081; c) J. Hamblin, L. J. Childs, N. W. Alcock, M. J. Hannon, *J. Chem. Soc. Dalton Trans.* **2002**, 164–169; d) L. J. Childs, N. W. Alcock, M. J. Hannon, *Angew. Chem.* **2002**, *114*, 4418–4421; *Angew. Chem. Int. Ed.* **2002**, *41*, 4244–4247; e) J. Hamblin, A. Jackson, N. W. Alcock, M. J. Hannon, *J. Chem. Soc. Dalton Trans.* **2002**, 1635–1641; f) A. Lavalette, F. Tuna, J. Hamblin, A. Jackson, G. Clarkson, N. W. Alcock and M. J. Hannon, *Chem. Commun.* **2003**, 2666–2667; g) F. Tuna, G. Clarkson, N. W. Alcock, M. J. Hannon, *J. Chem. Soc. Dalton Trans.* **2003**, 2149–2155; h) F. Tuna, J. Hamblin, G. Clarkson, W. Errington, N. W. Alcock, M. J. Hannon, *Chem. Eur. J.* **2002**, *8*, 4957–4964.

[10] M. J. Hannon, C. L. Painting, J. Hamblin, A. Jackson, W. Errington, *Chem. Commun.* **1997**, 1807–1808.

[11] a) M. J. Hannon, C. L. Painting, N. W. Alcock, *Chem. Commun.* **1999**, 2023–2024; b) L. J. Childs, Ph. D. Thesis, University of Warwick **2002**; c) C. L. Painting, Ph. D. Thesis, University of Warwick **1999**; see also: d) J. Keegan, P. E. Kruger, M. Nieuwenhuyzen, N. Martin, *Cryst. Growth Des.* **2002**, *2*, 329–332; e) C. He, C. Y. Duan, C. J. Fang, Q. J. Meng, *J. Chem. Soc. Dalton Trans.* **2000**, 2419–2424.

[12] F. Tuna, J. Hamblin, A. Jackson, G. Clarkson, N. W. Alcock, M. J. Hannon, *J. Chem. Soc. Dalton Trans.* **2003**, 2141- 2148.

[13] a) A. Bilyk, M. M. Harding, P. Turner and T. W. Hambley, *J. Chem. Soc. Dalton Trans.* **1994**, 2783–2790; b) C. O. Dietrich-Buchecker, J. F. Nierengarten, J. P. Sauvage, N. Armaroli, V. Balzani, L. DeCola, *J. Am. Chem. Soc.* **1993**, *115*, 11237–11244.

[14] M. J. Hannon, C. L. Painting, E. A. Plummer, L. J. Childs, N. W. Alcock, *Chem. Eur. J.* **2002**, *8*, 2226–2238.

[15] a) A. Marquis Rigault, A. Dupont Gervais, P. N. W. Baxter, A. Van-Dorsselaer, J.-M. Lehn, *Inorg. Chem.* **1996**, *35*, 2307–2310; b) P. N. W. Baxter, J.-M. Lehn, B. O. Kneisel, G. Baum, D. Fenske, *Chem. Eur. J.* **1999**, *5*, 113–120; c) P. N. W. Baxter, J.-M. Lehn, G. Baum, D. Fenske, *Chem. Eur. J.* **1999**, *5*, 102–112.

[16] a) C. Dietrich-Buchecker, M. C. Jimenez-Molero, V. Sartor, J.-P. Sauvage, *Pure Appl. Chem.* **2003**, *75*, 1383–1393; b) J. P. Collin, C. Dietrich-Buchecker, P. Gavina, M. C. Jimenez-Molero, J.-P. Sauvage, *Acc. Chem. Res.* **2001**, *34*, 477–487; c) J. C. Chambron, J.-P. Sauvage, *Chem. Eur. J.* **1998**, *4*, 1362–1366; d) P. N. W. Baxter, H. Sleiman, J.-M. Lehn, K. Rissanen, *Angew. Chem.* **1997**, *109*, 1350–1352; *Angew. Chem. Int. Ed. Engl.* **1997**, *36*, 1294–1296.

[17] a) H. Sleiman, P. N. W. Baxter, J.-M. Lehn, K. Airola, K. Rissanen, *Inorg. Chem.* **1997**, *36*, 4734–4742; b) H. Sleiman, P. Baxter, J.-M. Lehn, K. Rissanen, *J. Chem. Soc. Chem. Commun.* **1995**, 715–716.

[18] P. N. W. Baxter, G. S. Hanan, J.-M. Lehn, *Chem. Commun.* **1996**, 2019–2020.

[19] C. A. Hunter, J. K. M. Sanders, *J. Am. Chem. Soc.* **1990**, *112*, 5525–5534.

[20] M. Vázquez, M. , M. R. Bermejo, M. Fondo, A. M. González, J. Mahía,, L. Sorace, D. Gatteschi, *Eur. J. Inorg. Chem.* **2001**, 1863–1868.

[21] S. D. Reid, A. J. Blake, W. Köckenberger, C. Wilson, J. B. Love, *J. Chem. Soc. Dalton Trans.* **2003**, 4387–4388.

[22] In the box, two methylene protons (one from each ligand) point into the cavity of the box while the other two protons point towards the exterior of the box.

[23] For discussions of CH···π bonds see for example: a) T. Steiner, *Chem. Commun.* **1997**, 727–734; b) T. Steiner, *Chem. Commun.* **1999**, 313–314; c) G. R. Desiraju, *Acc. Chem. Res.* **1991**, *24*, 290–296; d) G. R. Desiraju, *Acc. Chem. Res.* **1996**, *29*, 441–449. For

CH···π bonds as a supramolecular control element see for example: e) K. N. Houk, S. Menzer, S. P. Newton, F. M. Raymo, J. F. Stoddart, D. J. Williams, *J. Am. Chem. Soc.* **1999**, *121*, 1479–1487; f) J. M. A. Robinson, D. Philp, B. M. Kariuki, K. D. M. Harris, *Chem. Commun.* **1999**, 329–330; g) V. R. Thalladi, H. C. Weiss, D. Blaser, R. Boese, A. Nangia, G. R. Desiraju, *J. Am. Chem. Soc.* **1998**, *120*, 8702–8710, and references therein.

[24] L. J. Childs, M. J. Hannon, N. W. Alcock, *Angew. Chem.* **2002**, *114*, 4418–4420; *Angew. Chem. Int. Ed.* **2002**, *41*, 4244–4247.

[25] Fluxional behaviour is common in acteonitrile solution for copper(I) systems and this is reflected in dramatically lower stability constants for copper(I) bipyridines and pyridylimines in acetonitrile than in other solvents. See ref. [9] for examples of such fluxional behaviour.

[26] For examples of circular helicates see ref [2] and a) P. L. Jones, K. J. Byrom, J. C. Jeffery, J. A. McCleverty and M. D. Ward, *Chem. Commun.* **1997**, 1361–1362; b) J. S. Fleming, K. L. V. Mann, C. A. Carraz, E. Psillakis, J. C. Jeffery, J. A. McCleverty and M. D. Ward, *Angew. Chem.* **1998**, *110*, 1315–1318; *Angew. Chem. Int. Ed.* **1998**, *37*, 1279–1281; c) G. Baum, E. C. Constable, D. Fenske, C. E. Housecroft, T. Kulke, *Chem. Commun.* **1999**, 195–196; d) C. S. Campos-Fernàndez, R. Clérac, K. R. Dunbar, *Angew. Chem.* **1999**, *111*, 3685–3688; *Angew. Chem. Int. Ed.* **1999**, *38*, 3477–3479; e) T. Bark, M. Düggeli, H. Stoeckli-Evans, A. von Zelewsky, *Angew. Chem.* **2001**, *113*, 2924–2927; *Angew. Chem. Int. Ed.* **2001**, *40*, 2848–2851; f) O. Mamula, A. vonZelewsky, G. Bernardinelli, *Angew. Chem.* **1998**, *110*, 301–305; *Angew. Chem. Int. Ed.* **1998**, *37*, 290–293; g) O. Mamula, F. J. Monlien, A. Porquet, G. Hopfgartner, A. E. Merbach, A. von Zelewsky, *Chem. Eur. J.* **2001**, *7*, 533–539; h) C. Provent, E. Rivara-Minten, S. Hewage, G. Brunner, A. F. Williams, *Chem. Eur. J.* **1999**, *5*, 3487–3494; i) G. Hopfgartner, C. Piguet, J. D. Henion, *J. Am. Soc. Mass Spectrom.* **1994**, *5*, 748–756.

[27] G. M. Sheldrick, *Acta Crystallogr. Sect A*, **1990**, *46*, 467.

[28] SMART user's manual, Siemens Industrial Automation Inc., Madison, WI, **1994**.

[29] J. Cosier and A. M. Glazer, *J. Appl. Crystallogr.* **1986**, *19*, 105.

Received: February 19, 2004
Published online: July 19, 2004

